

Chapter 6

Massive expansion of marine Archaea during a mid-Cretaceous oceanic anoxic event

Marcel M.M. Kuypers, Peter Blokker, Jochen Erbacher, Hanno Kinkel, Richard D. Pancost, Stefan Schouten, Jaap S. Sinninghe Damsté

Published in *Science*, 293, 92-94, 2001

Abstract

Biogeochemical and stable carbon isotopic analysis of black shale sequences deposited during an Albian oceanic anoxic event (~112 Myr) indicate that up to 80 wt. % of sedimentary organic carbon is derived from marine, non-thermophilic archaea. The ^{13}C content of archaeal molecular fossils indicates that these archaea were living chemoautotrophically. Their massive expansion may have been a response to the strong stratification of the ocean during this anoxic event. In fact, the sedimentary record of archaeal membrane lipids suggests that this anoxic event actually marks a moment in Earth history at which certain hyperthermophilic archaea adapted to low-temperature environment.

6.1 Introduction

The mid-Cretaceous was a period of exceptional oceanic volcanic activity. Evidence of this igneous activity is provided by the presence of large oceanic plateau, including the Ontong Java, Kerguelen and Caribbean Plateau, which have been dated at 125-88 Myr (1). Enhanced volcanic outgassing of CO₂ could have caused the mid-Cretaceous ‘greenhouse’ climate (2), with its minimal equator-to-pole temperature difference. In contrast, episodic oceanic anoxic events (OAEs) may have effectively reduced CO₂ concentrations during brief periods by sequestering carbon in the subsurface (3, 4). The widespread deposition of black-shales during the OAEs has been attributed either to decreased organic matter (OM) remineralisation resulting from a decreased oxygen flux (5) or to increased primary productivity overwhelming the oxic OM remineralisation potential of the water column (6). The increase in organic carbon (OC) accumulation rates during the OAEs in these two basically different models is attributed to enhanced burial of marine OM, which is typically of phytoplanktonic origin. Here we determined the source for both soluble and insoluble OM of the early Albian OAE 1b black shales of the Ocean Drilling Program site 1049C (North Atlantic Ocean off the coast of Florida: 30°08’N, 76°06’W) and the Ravel section of the Southeast France Basin (44°06’N, 6°28’E) using optical, chemical, and stable carbon isotopic analyses, and show that the sources of OM for this OAE are fundamentally different from other OAEs.

6.2 Results and discussion

The upper Aptian-lower Albian sequence of site 1049C consists of marls and calcareous marls characterised by a low (< 0.1 wt%) OC content interrupted by an OC-rich (up to 6 wt%; Fig. 1A) black shale interval. This black shale interval (grey shaded area; Fig. 1) has been identified as the local expression of OAE 1b (7). The bulk OC shows a sharp increase in its ¹³C-content during the OAE1b (Fig. 1B). Similar increases in δ¹³C values observed for marine carbonates and OM from other mid Cretaceous OAEs have been attributed to an increase in the ¹³C content of the oceanic/atmospheric pool of inorganic carbon as a result of globally enhanced OC burial rates (3). However, the stable carbon isotopic composition of picked planktonic and benthic foraminifers (7) indicate that there was no significant increase in δ¹³C values for inorganic carbon during the OAE1b at site 1049C.

To resolve the origin of the increase in δ¹³C values for bulk OC (δ¹³C_{org.}) we first analysed the extractable OM. The saturated hydrocarbon fractions of the black shales contain long-chain (C₂₅-C₃₁) *n*-alkanes that are largely derived from leaf waxes of terrestrial plants, some bacterial hopanoids and acyclic isoprenoids. Remarkably, the acyclic isoprenoid, 2,6,15,19-tetramethylcosane [TMI (I), Fig. 1] is the most abundant component of the saturated hydrocarbon fraction. So far, TMI has only been found in the contemporaneous (7) OAE1b black shale of the Ravel section in France (8). TMI (I) is structurally closely related to 2,6,10,15,19-pentamethylcosane (PMI) (II), a compound of known archaeal origin (9), which was also present in the saturated hydrocarbon fraction. Further evidence for archaeal compounds was found on

treating the polar fraction from the black shale interval with HI/LiAlH_4 to cleave ether bonds. The released fractions were dominated by acyclic (**a**), monocyclic (**b**), bicyclic (**c**) and tricyclic (**d**)

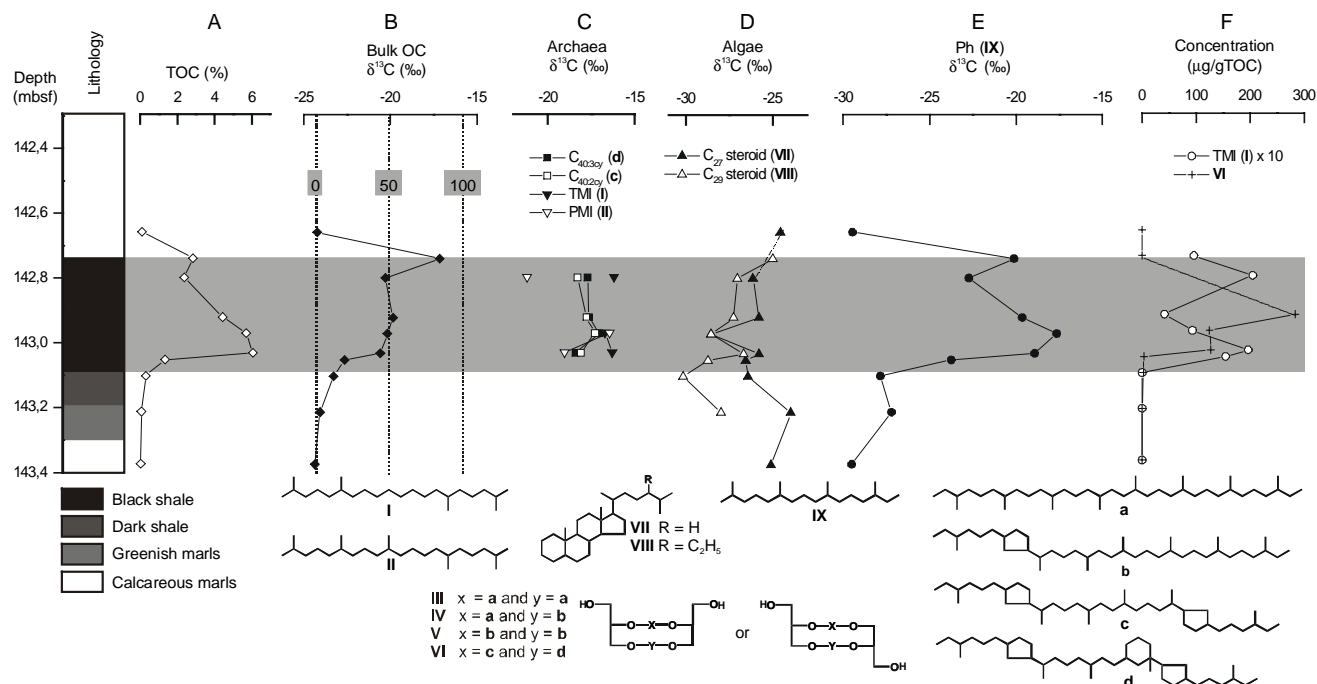


Figure 1 Stratigraphy, bulk and biomarker data of Ocean Drilling Project site 1049C. TOC content (A), and carbon isotope values (in ‰ vs. VPDB) of bulk OC (B), bi- ($\text{C}_{40:2\text{cy}}$) and tricyclic ($\text{C}_{40:3\text{cy}}$) biphytanes, PMI (II) and TMI (I) derived from archaea (C), oxygen-bound steranes [cholestane (VII) and 24-ethyl-cholestane (VIII)] mainly derived from marine algae (D), and oxygen-bound phytane (IX) derived either from the isotopically ‘light’ (^{12}C -rich) phytol side-chain (VI) of algal and cyanobacterial chlorophyll or the isotopically ‘heavy’ (^{13}C -rich) archaeal membrane lipids (E), and concentrations ($\mu\text{g}/\text{gTOC}$) of GDGT VI and TMI derived from archaea (F) of late Aptian/early Albian abyssal sediments from site 1049C (28). In all graphs the centre of the bullet corresponds to the top of the ~2 cm thick sediment samples. The OAE1b black shale interval has been indicated as a grey shaded area in the graphs. Dotted lines in graph (B) indicate estimated contributions (in %) of archaeal derived insoluble OM to TOC as discussed in text. Relevant structures are indicated.

biphytanes (C_{40} isoprenoids), which are also exclusively found in archaea (10, 11). In addition, a recently developed HPLC/MS technique (12) revealed the presence of four (III–VI) intact isoprenoid glycerol dialkyl glycerol tetraethers (GDGTs) in the black shale interval. GDGTs are the main constituents of archaeal membranes (11) and IV–V are characteristic of the archaeal lineage Crenarchaeota (10, 13), which includes the hyperthermophilic archaea which thrive at temperatures $>60^\circ\text{C}$. In contrast, VI is highly diagnostic for their non-thermophilic relatives (11, 14–16), and the dominance of this compound (representing 60% of total GDGTs) indicates an important input of non-thermophilic crenarchaeota. To the best of our knowledge this is the earliest fossil evidence for marine non-hyperthermophilic crenarchaeota, extending their geological record by more than 60 million years (14).

The $\delta^{13}\text{C}$ values of components of unambiguous archaeal origin such as II, c and d and the related I are significantly enriched in ^{13}C relative to algal steroids VII–VIII (Fig. 1C–D), bacterial derived hopanes and the leaf-wax *n*-alkanes *n*- C_{29} and *n*- C_{31} from higher plants (17). Cholestane

(**VII**) and 24-ethyl-cholestane (**VIII**), released after HI/LiAlH₄ treatment, derive from C₂₇ and C₂₉ sterols, predominantly biosynthesised by marine algae (18). Their $\delta^{13}\text{C}$ values record changes in the stable carbon isotopic composition of algae (Fig. 1C). The offset of >10‰ between the $\delta^{13}\text{C}$ values for TMI/PMI and the algal biomarkers (Figs. 1C-D) is in agreement with our earlier observations for the OAE1b black shales of the Ravel section in France (8).

While archaeal lipids are abundant in the OC-rich OAE1b black shales, they are largely absent in the adjacent sediments (Fig. 1F). This suggests a significantly increased archaeal contribution to the sedimentary OM during OAE1b. Evidence for an increase in the relative contribution of archaeal biomass is also provided by the ~12‰ shift in $\delta^{13}\text{C}$ values for the isoprenoid phytane (**IX**) released from the polar fractions upon HI/LiAlH₄ treatment (Fig. 1E). Phytane (**IX**) derives either from the isotopically ‘light’ (¹²C-rich) phytol side-chain of algal and cyanobacterial chlorophyll or the isotopically ‘heavy’ (¹³C-rich) archaeal membrane lipids such as archaeol. Before and after the black shale interval, $\delta^{13}\text{C}$ values for phytane (**IX**) are comparable to those of steranes, consistent with an algal origin, whereas in the black shale interval it is enriched by up to 12‰, indicating a predominant archaeal origin. There is no coinciding positive shift in $\delta^{13}\text{C}$ values for the algal steranes (Fig. 1D). Therefore, the sharp increase in $\delta^{13}\text{C}$ values for phytane (**IX**) indicates a change in the relative contribution from algal and archaeal OM sources during the OAE1b. An increase in the relative contribution of ¹³C enriched archaeal biomass to the OM deposited during OAE1b could thus also explain the shift in $\delta^{13}\text{C}$ values for bulk OC (Fig. 1B).

To determine the archaeal contribution to the bulk OM, the insoluble OM, representing >95% of the bulk OM, was also investigated. Thin laminae of amorphous OM (as revealed by scanning electron microscopy) that occur throughout the black shale make up a significant part of the OM. This OM cannot be hydrolysed either by strong acid or base, and shows the enrichment in ¹³C ($\delta^{13}\text{C} = -15.5\text{‰}$) typical of archaeal lipids. Both thermal (flash pyrolysis) and chemical degradation (RuO₄ oxidation) of this amorphous OM almost exclusively (>95%) releases molecules with acyclic isoprenoidal carbon skeleton. These isoprenoids were also abundant in the flash pyrolysates of the OAE1b black shale of the Ravel section (8, 19). The weighted average of the $\delta^{13}\text{C}$ values of the chemically released isoprenoids ($\delta^{13}\text{C} = -14\text{‰}$) from the black shale is in good agreement with the bulk isotopic composition of the OC from the laminae, indicating that these are the main components of this polymeric OM. The distribution of chemical degradation products indicates that the polymer consists of monomers with essentially two different carbon skeletons: TMI (**I**) and PMI (**II**) linked together by ether-bonds [Kuypers et al., unpublished results]. This strongly suggests that the positive shift in $\delta^{13}\text{C}_{\text{org}}$ (Fig. 1B) indeed results from an increased contribution of ¹³C enriched archaeal-derived OC during OAE1b.

The relative contribution of archaeal polymer to the OC can be estimated from $\delta^{13}\text{C}_{\text{org}}$ using a two end-member mixing model and assuming that the $\delta^{13}\text{C}$ value (~ -24‰) for bulk sedimentary OC before the OAE1b represents the non-archaeal endmember and $\delta^{13}\text{C} = -15.5\text{‰}$ for the archaeal endmember. There is on average a very large (~50 wt%) and sometimes even a predominant (~80 wt%) contribution of archaeal OC in the black shale interval (Fig. 1B). A significant contribution (up to 40 wt%) of archaeal OC is also found for the OAE1b black shales in France using the stable carbon isotopic composition of *n*-alkanes and isoprenoids obtained after off-line pyrolysis of the

bulk OM (19) as algal and archaeal endmembers, respectively. Although prokaryotes can constitute more than 70 wt% of carbon biomass in the upper ocean (20) and their biomarkers are abundantly present in the sediment (21), evidence for a substantial (>10 %) prokaryotic contribution to Phanerozoic OC-rich sediments is generally lacking (22). Therefore, the domination of OM derived from archaea during OAE1b is both unexpected and unprecedented, indicating that this was a unique time in Earth history. Certainly, it reveals that enhanced OM deposition during OAE1b was caused by a different mechanism than has been invoked for other OAEs.

The diversity of archaeal lipids recovered from the OAE1b black shales suggests that they derive from a multitude of archaeal species. However, the specific ^{13}C enrichment of these lipids indicates a common 'heavy' (^{13}C -rich) carbon source for the archaea and/or a common pathway of carbon-fixation with a reduced ^{13}C fractionation effect compared to the Calvin cycle used by algae, cyanobacteria and higher plants. The large enrichment (up to 12 ‰) in $^{13}\text{C}/^{12}\text{C}$ ratios between the algal biomarkers and the archaeal molecular fossils suggest that archaea were not living heterotrophically on photoautotrophic biomass. Hence it seems likely that the archaea present during OAE1b were autotrophs and used a chemical energy source for carbon fixation. The ecological niche of these chemoautotrophic archaea in the mid-Cretaceous ocean is not clear.

The abundance of GDGT **VI** in the OAE1b black shales can be interpreted, however, to suggest that at least some of these archaea were thriving in the marine water column. In the present-day ocean GDGT **VI** is abundantly present in marine particulate OM and surface sediments (11, 16), which is consistent with the fact that planktonic representatives of the marine crenarchaeota comprise as much as 20% of the picoplankton (23). Compound-specific radiocarbon analyses of biphytanes **c** and **d** derived from **VI** indicate that these archaea are not feeding on phytoplanktonic biomass but rather use 'old' ^{14}C -depleted dissolved inorganic carbon from well below the photic zone in the water column (24). Furthermore, these components show a significant ^{13}C enrichment (4-5‰) relative to algal steroids (14), indicating that planktonic crenarchaeota, like related hyperthermophiles (25), may use a non-Calvin cycle pathway of carbon assimilation with a smaller degree of carbon-isotope fractionation during carbon assimilation. The offset between $\delta^{13}\text{C}$ values for the biphytane **d** derived from **VI** in present-day marine particulate OM (-20 to -23‰) (14) and in OAE1b sediments (-17 to -18‰) can be explained by the enrichment of dissolved inorganic carbon in ^{13}C by 2-3‰ relative to modern values during the mid-Cretaceous (2). The remainder of the larger (3-7‰) enrichment of biphytane **d** relative to algal steroids can probably be accounted for by enhanced carbon isotope fractionation by algae during the mid-Cretaceous due to enhanced CO_2 availability (26). Carbon isotopic evidence thus suggests that the mid-Cretaceous crenarchaeota producing GDGT **VI** used similar biochemical pathways as their present-day representatives.

The massive expansion of marine, non-thermophilic archaea during the mid-Cretaceous OAE1b is unprecedented and could actually mark a moment in geological history at which certain hyperthermophilic archaea adapted to low-temperature environments. Older sediments of comparable thermal maturity do not contain the characteristic GDGT **VI**, whereas this GDGT is commonly found in black shales younger than Albian (11, 14). On the other hand, TMI (**I**) and macromolecular OM composed thereof has so far only been reported for this time interval. This suggests that at least two distinct groups of marine, non-thermophilic archaea existed, of which one has thrived for the past 112 Myr, whereas the other (TMI-producing) group seems to become

extinct after OAE1b when environmental conditions became less favourable. Prolonged (millions of years) periods of enhanced hydrothermal activity (1) would have significantly altered the ocean chemistry during the mid-Cretaceous, providing the necessary reduced compounds to sustain a large community of chemoautotrophic archaea. In fact, the Cretaceous strontium isotope record indicates maximum ocean-ridge crustal production during the Aptian-early Albian stages (27). In addition, the pronounced water column stratification and anoxic conditions that are characteristic for OAE1b (7) may have assisted in the development of a diverse community of marine, chemoautotrophic, non-thermophilic archaea.

6.3 References and Notes

1. R. L. Larson, *Geology* **19**, 547 (1991).
2. M. A. Arthur, W. E. Dean, S. O. Schlanger, *Amer. Geophys. Union Monogr.* **32**, 504 (1985).
3. M. A. Arthur, W. A. Dean, L. M. Pratt, *Nature* **335**, 714 (1988).
4. M. M. M. Kuypers, R. D. Pancost, J. S. Sinninghe Damsté, *Nature* **399**, 342 (1999).
5. T. J. Bralower and H. R. Thierstein, *Geol. Soc. Spec. Publ.* **26**, 345 (1987).
6. S. O. Schlanger and H. C. Jenkyns, *Geol. Mijnb.* **55**, 179 (1976).
7. J. Erbacher, B. T. Huber, R. D. Norris, M. Markey *Nature* **409**, 325 (2001).
8. A. Vink, S. Schouten, S. Sephton, J. S. Sinninghe Damsté, *Geochim. Cosmochim. Acta* **62**, 965 (1998).
9. S. Schouten, M. J. E. C. van der Maarel, R. Huber, J. S. Sinninghe Damsté, *Org. Geochem.* **26**, 409 (1997).
10. M. De Rosa and A. Gambacorta, *Prog. Lipid Res.* **27**, 153 (1988).
11. S. Schouten, E. C. Hopmans, R. D. Pancost, J. S. Sinninghe Damsté, *Proc. Nat. Acad. Sci. USA* **97**, 14421 (2000).
12. E. C. Hopmans, S. Schouten, R. D. Pancost, M. T. J. van der Meer, J. S. Sinninghe Damsté, *Rapid. Commun. Mass Spectrom.* **14**, 585 (2000).
13. K. O. Stetter, in *Extremophiles: Microbial Life in Extreme Environments*, K. Horikoshi and W. D. Grant, Eds. (Wiley-Liss, Inc., New York, 1998), Chap. 1.
14. M. J. L. Hoefs et al., *Appl. Environ. Microbiol.* **63**, 3090 (1997).
15. E. F. DeLong et al., *Appl. Environ. Microbiol.* **64**, 1133 (1998).
16. Recent direct HPLC-MS analyses of a uni-archaeal culture of the non-thermophilic crenarchaeotum *Cenarchaeum symbiosum* (kindly provided by Dr. E.F. DeLong) and marine particles from the marine water column have indicated that VI is one of the most abundant lipids present (Schouten, Hopmans and Sinninghe Damsté, unpublished results).
17. For supplementary material is available see appendix
18. J. K. Volkman, *Org. Geochem.* **9**, 83-99 (1986).
19. I. M. Höld, S. Schouten, H. M. E. van Kaam-Peters, J. S. Sinninghe Damsté, *Org. Geochem.* **28**, 179 (1998).
20. J. A. Fuhrman, T. D. Sleeter, C. A. Carlson, L. M. Proctor, *Mar. Ecol. Progr. Ser.* **57**, 207 (1989).
21. G. Ourisson and P. Albrecht, *Acc. Chem. Res.* **25**, 398 (1992).
22. J. S. Sinninghe Damsté and S. Schouten, *Org. Geochem.* **26**, 517 (1997).
23. M. B. Karner, E. F. DeLong, D. M. Karl, *Nature* **409**, 507 (2001).
24. A. Pearson, T. I. Eglinton, A. P. McNichol, B. C. Benitez-Nelson, J.M. Hayes, *Geochim. Cosmochim. Acta*, in press.
25. M. T. J. van der Meer, S. Schouten, W. I. C. Rijpstra, G. Fuchs., J. S. Sinninghe Damsté, *FEMS Microbiol. Lett.*, in press.
26. M. A. Arthur, W. E. Dean, G. E. Claypool, *Nature* **315**, 216 (1985).
27. T. J. Bralower, P. D. Fullager, C. K. Paull, G. S. Dwyer, R. M. Leckie *GSA Bull.* **109**, 1421 (1997).
28. Total Organic Carbon (TOC) contents were determined using a CN analyser. The $\delta^{13}\text{C}$ values ($\pm 0.1\text{‰}$) ($\delta^{13}\text{C} = [(\text{R}_{\text{sample}}/\text{R}_{\text{standard}} - 1) \cdot 1,000]$, where R is $^{13}\text{C}/^{12}\text{C}$ and the standard the Vienna Pee Dee belemnite) were measured

on bulk sediments after removal of the inorganic carbonates with diluted HCl using automated on-line combustion followed by conventional isotope ratio-mass spectrometry. The powdered samples (15 to 30 g) were Soxhlet extracted for *c.* 24 h to obtain the total lipid fraction. The total extracts were separated into apolar and polar fractions using column chromatography. The hydrocarbons that were released from the polar fraction by HI/LiAlH₄ and subsequent hydrogenation were isolated using column chromatography. Samples were analysed by GC-mass spectrometry (GC-MS) for identification. Compound-specific $\delta^{13}\text{C}$ analyses were performed using GC-isotope-ratio-monitoring MS. The $\delta^{13}\text{C}$ values for individual compounds are the means of duplicate runs ($\delta^{13}\text{C} = \pm 0.3$ to 0.6) expressed versus VPDB. HPLC/MS analyses were performed as previously described (12). Macromolecular material was isolated from the decalcified and extracted sediments by density centrifugation (at 3700 r.p.m. for 5 min) using pure dichloromethane (floating fraction). Fourier transform infrared spectroscopy (frequency range of 400 cm⁻¹ to 4000 cm⁻¹) was performed on 2 mg of dry macromolecular material pressed into KBr pellets. The extract obtained after RuO₄ degradation of ~5 mg of isolated macromolecular material was derivatised with BF₃/methanol prior to analysis. Curie-point flash pyrolysis (10 s; 610°C) was performed with a pyrolysis unit connected to a gas chromatograph.

29. We thank A. Boom for helpful discussions; R. Kloosterhuis, P. Slootweg, M. Dekker, M. Kienhuis, E.C. Hopmans and W. Pool, for analytical assistance; and the Ocean Drilling Program for providing the samples. The investigations were supported by the Research Council for Earth and Life sciences (ALW) with financial aid from the Netherlands Organisation for Scientific Research (NWO).

Appendix

Source organism	Biochemical Precursor	C skeleton	Mode	$\delta^{13}\text{C}$ (‰)
Higher plants	<i>n</i> -C ₂₇	<i>n</i> -C ₂₇	Free	-27.7 to -28.9
	<i>n</i> -C ₃₁	<i>n</i> -C ₃₁	Free	-27.7 to -28.0
Algae/higher plants	24-ethyl-cholesterols	C ₂₉ sterane (VIII)	Alc.	-25.1 to -30.2
Algae	24-methyl-cholesterols	C ₂₈ sterane	Alc.	-27.0 to -29.2
Algae/zooplankton	Sterols	C ₂₇ sterane (VII)	Alc.	-23.9 to -28.5
Algae/cyanobact.	Chlorophyll	Phytane (IX)	Alc.	-27.2 to -29.5
Heterotr./cyanobact.	Bacteriohopanepolyols	C ₂₉ hopane	Free	-23.7 to -24.9
	Bacteriohopanepolyols	C ₃₁ hopane	Free	-26.1 to -27.0
Archaea/bacteria	Squalane/squalene	Squalane	Free	-17.6 to -23.4
Archaea	GDGTs (III , IV)	C _{40:1cycl. (b)}	E-bd/alc.	-17.6 to -20.0
	GDGTs (V)	C _{40:2cycl. (c)}	E-bd/alc.	-17.1 to -18.4
	GDGTs (VI)	C _{40:3cycl. (d)}	E-bd/alc.	-17.3 to -18.3
	Archaeol	Phytane (IX)	E-bd.	-17.7
	PMI (II)/unsat. PMI	PMI (II)	Free	-16.5 to -21.2
	Unknown	TMI (I)	Free	-16.2 to -16.7
	Funct. TMI/PMI	TMI/PMI	E-bd	-13.1 to -15.0

Source organisms, inferred biochemical precursor, isotopic composition and mode of occurrence of C skeletons encountered in the sediment. Carbon skeletons are shown in Fig. 1. Carbon skeletons occur in the following modes: free hydrocarbons (free), macromolecularly S-bound moiety (S-bd), alcohols (Alc.) and ether-bound moiety (E-bd). The range of measured stable carbon isotopic values for individual components is indicated. Abbreviations are isopr., isoprenoid alkanes; 1cycl., mono cyclic; Funct., functionalised; unsat., unsaturated; Heterotr., heterotrophic bacteria; cyanobact., cyanobacteria.